NANO LETTERS

2006
Vol. 6, No. 4
769−773

Ion Coordinating Sensitizer for High Efficiency Mesoscopic Dye-Sensitized Solar Cells: Influence of Lithium Ions on the Photovoltaic Performance of Liquid and Solid-State Cells

Daibin Kuang, Cedric Klein, Henry J. Snaith, Jacques-E Moser, Robin Humphry-Baker, Pascal Comte, Shaik M. Zakeeruddin,* and Michael Grätzel*

Laboratory for Photonics and Interfaces, Institute of Chemical Sciences and Engineering, Ecole Polytechnique Fédérale de Lausanne, 1015 Lausanne, Switzerland

Received January 12, 2006; Revised Manuscript Received February 20, 2006

ABSTRACT

A Li^+ coordinating sensitizer, NaRu(4-carboxylic acid-4′-carboxylate)(4,4′-bis[(triethylene glycol methyl ether) methyl ether]-2,2′-bipyridine)-$(NCS)_2$ (coded as K51), has been synthesized, and the effect of Li^+ coordination on its performance in mesoscopic titanium dioxide dye-sensitized solar cells has been investigated. Fourier transform infrared spectra suggest that Li^+ coordinates to the triethylene oxide methyl ether side chains on the dye molecules. With the addition of Li^+ to a nonvolatile liquid electrolyte, we observe a significant increase in the photocurrent density, with only a small decrease in the open-circuit voltage, contrary to a non ion coordinating dye which displays a large drop in potential with the addition of Li^+. For a solar cell incorporating an organic hole-transporter, we find the potential rises with increasing the Li^+ concentration in the hole-transporter matrix. For the liquid electrolyte and solid-state cells, we obtain power conversion efficiencies of 7.8% and 3.8%, respectively, under simulated sunlight.

In the search of alternative energy sources, dye-sensitized solar cells (DSCs) have attracted much attention due to their low cost and high efficiency.[1−3] Under operation, dye molecules, adsorbed to the surface of a mesoscopic TiO_2 film, inject photogenerated electrons into the conduction band of the metal oxide. The oxidized dye cations are then regenerated by electron donation from a redox electrolyte or, alternatively, hole injection into an organic hole-transporting material (HTM), for the solid-state analogy. The injected electrons may be transported to an external circuit by diffusion through the TiO_2 film or may be recaptured by the oxidized dye or the redox electrolyte/the hole in the HTM. The sensitizer plays a crucial role not only because it harvests sunlight and generates electric charges but also because it impairs interfacial charge recombination, being an insulator in the ground state.[4,5] Polypyridyl ruthenium complexes have proven to be the most efficient sensitizers to date, in comparison to organic dyes and other metal complexes used in DSCs.[6−16]

The influence of various cations added to the electrolyte upon the photovoltaic performance of DSCs has been well investigated.[17−21] Due to the small size of the Li^+, studies have revealed that it intercalates or strongly adsorbs to the surface of TiO_2. The surface adsorption results in a positive shift of the TiO_2 conduction band and consequently causes a dramatic drop in the open-circuit voltage of the cell. Ethylene oxide can form coordinative bonds with metal ions, and poly(ethylene oxide) (PEO) has been used for a quasi-solid-state DSC where the polymer acts as an ion transporting matrix.[22,23] Here, we prepared a novel ruthenium sensitizer by tethering the triethylene oxide methyl ether (TEOME) on the 4,4′ position of a 2,2-bipyridine ligand to introduce ion coordinating properties to the complex. We investigated the influence of different Li^+ concentrations, in the electrolyte solution, comparing the ion coordinating sensitizer (K51) with a non ion coordinating analogue (Z907), which has been previously reported. The molecular structures of the two dyes are shown in Figure 1. In the case of the K51 sensitizer there is small drop in the open-circuit voltage accompanied by a large increase in the photocurrent density with the addition of Li^+. A device using Z907 sensitizer also shows an increase in photocurrent; however, it exhibits a significant drop in potential. We attribute the potential invariance of the cell containing the K51 dye to be due to inhibition of Li^+ adsorption to the TiO_2 surface by coordination of Li^+ to the TEOME groups of the K51 sensitizer.

* To whom correspondence should be addressed. E-mail address: shaik.zakeer@epfl.ch; michael.graetzel@epfl.ch.

10.1021/nl060075m CCC: $33.50
Published on Web 03/18/2006

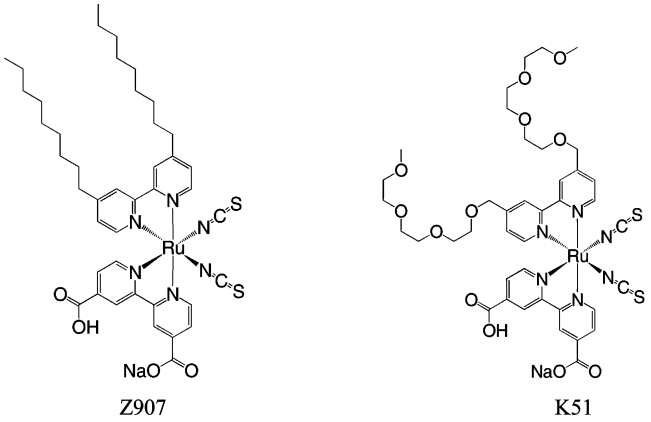

Figure 1. The molecular structure of Z907 and K51 dyes.

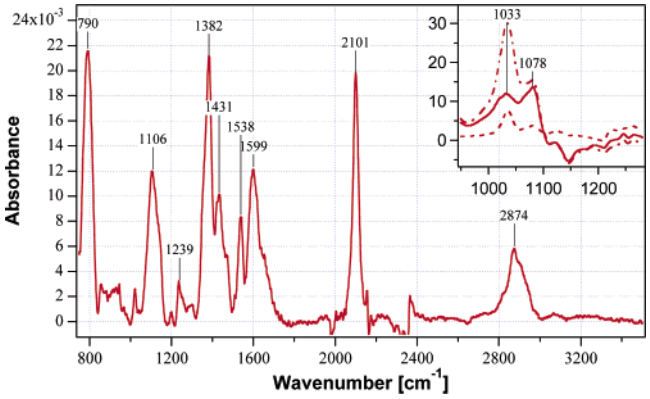

Figure 2. The ATR-FTIR spectrum of K51 dye adsorbed on 6 μm thick mesoscopic TiO_2 film. The spectrum from a TiO_2 reference film heated to 500 °C has been subtracted. The inset shows the difference spectra after the addition of 0.25 M LiI in acetonitrile solution. The solid curve is immediately after addition and the dot dashed after 5 min. The dashed line is obtained after washing with pure acetonitrile.

The K51 dye was prepared as described in Scheme 1, and a detailed synthesis and characterization is given in the Supporting Information.

Attenuated total reflection Fourier transform infrared (ATR-FTIR), luminescence, nanosecond laser transient-absorbance measurements, photocurrent and photovoltaic and electrochemical studies were preformed as reported in our earlier publications.[24−26] The dye-sensitized solar cells with liquid electrolytes used in this study were fabricated by identical methods as previously described with a double layer TiO_2 film consisting of a transparent layer of 10 μm thick (20 nm nanoparticles) and scattering layer of 4 μm (400 nm nanoparticles).[25] The film porosity was 60%. The composition of electrolytes is as follows. Electrolyte **A** contains 0.6 M 1-propyl-2,3-dimethylimidazolium iodide, 0.10 M I_2, and 0.5 M *N*-methylbenzimidazole in 3-methoxypropionitrile solvent. Electrolytes **B**, **C**, and **D** contain 0.05, 0.125, and 0.25 M $LiClO_4$ in electrolyte A, respectively. The solid-state devices were fabricated with approximately 2 μm thick mesoscopic TiO_2 films.[27]

The redoxpotential of K51 dye attached to the TiO_2 film was measured by cyclic voltammetry, and the band gap was determined by UV−vis absorption and emission spectroscopy (shown as Figures S1 and S2 in the Supporting Information). The formal redox potential of K51 dye adsorbed to the surface of TiO_2 film was found to be 1.09 V vs NHE. The E_{0-0} transition energy was estimated[28] to be 1.80 eV, and thus $\phi^0(S^+/S^*)$ of K51 was calculated to be −0.71 V vs NHE.

The excited-state lifetime of K51 (absorbing at 620 nm) was determined by transient absorbance measurements to be 11 ns. As the electron injection from the exited state dye is in the femtosecond range, the lifetime of the exited state measured is sufficient to produce near quantitative injection of electrons into the TiO_2 electrodes.

ATR-FTIR has been demonstrated to be a powerful technique to reveal structural information of metal complexes adsorbed onto TiO_2 surfaces.[29] Figure 2 shows the ATR-FTIR spectrum of K51 dye adsorbed on the surface of the mesoscopic TiO_2 film, corrected by subtracting a spectrum of a "blank" TiO_2 reference film. The strong signal peak at 2101 cm^{-1} is attributed to the N-coordinated thiocyanate group (υ(CN)). The peaks at 1382 and 1599 cm^{-1} arise from the symmetric and asymmetric stretching modes of carboxylate groups ($\upsilon(COO^-_s)$). The sharp peak located at 1538 cm^{-1} is ascribed to bipyridyl modes, and the peaks observed at 2874 and 2935 (sh) cm^{-1} are due to the symmetric and asymmetric stretching modes of the CH_2 units of the ethylene oxide chains. The medium broad peak at 1106 cm^{-1} is

Scheme 1 [a]

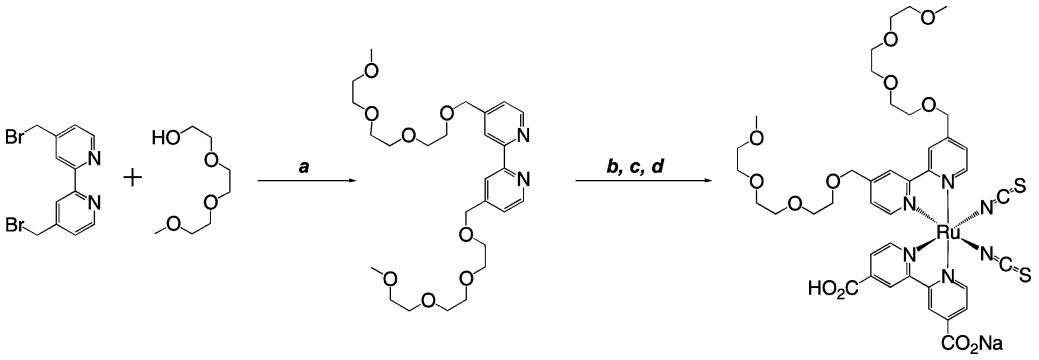

[a] Key: (*a*) NaH, THF, Δ. (*b*) $[Ru(p\text{-cymene})Cl_2]_2$, EtOH, Δ. (*c*) 4,4′-dicarboxy-2,2′-bipyridine, DMF 140 °C. (*d*) NH_4NCS·DMF, 140 °C.

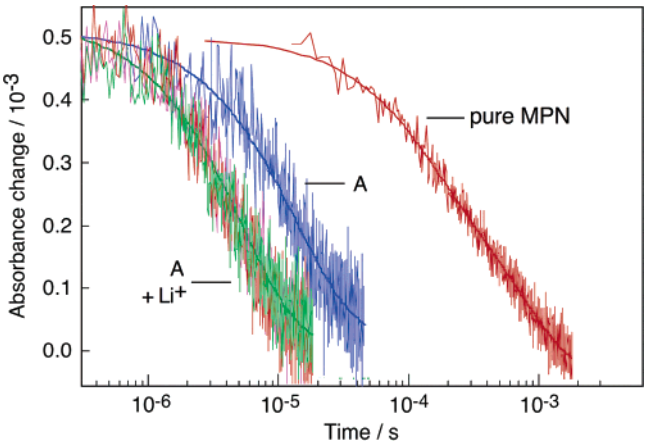

Figure 3. Transient absorbance decay kinetics of the oxidized state of K-51 dye adsorbed on mesoscopic TiO_2 films in pure 3-methoxypropionitrile redox-inactive solvent and in the presence of electrolyte **A**. Three decay curves were obtained at shorter time scale in the presence of electrolyte **A** with 0.05, 0.125, and 0.25 M $LiClO_4$ added, which are practically superimposed. Absorbance changes were measured at a probe wavelength of 680 nm upon 600 nm pulsed laser excitation (5 ns fwhm pulse duration, 25 $\mu J \cdot cm^{-2}$ pulse fluence, 30 Hz repetition rate). Signals were obtained by typically averaging over 3000 laser shots. Solid curves drawn through the experimental data are double exponential fits.

derived from the υ(C−O) stretch of the poly(ethylene oxide) group. The broadness of the latter peak signifies the disordered nature of these chains.

The K51 dye adsorbed to the surface of TiO_2 film was exposed to a solution of 0.25 M lithium iodide in acetonitrile, and the changes in IR spectrum were monitored. In the region of the υ(C−O) stretch at 1106 cm^{-1} there is a shift to lower energy (1078 cm^{-1}) due to coordination with lithium ions (C−O···Li^+).[30] The peak at 1033 cm^{-1} is due to the acetonitrile solvent. Since the υ(C−O) peak (Li^+ free) at 1106 cm^{-1} is diminished by approximately 50% in the presence of Li^+, we estimate an average of one Li^+ is associated with each dye under these conditions (there are two TEOME chains per molecule). After the film is rinsed with pure acetonitrile, the original peaks are restored.

Kinetic competition between back electron transfer from the conduction band of TiO_2 to the dye cations (S^+) and the interception of the oxidized species of the sensitizer by the redox mediator to a large extent controls the photon-to-current efficiency of the photovoltaic device. We have scrutinized the dynamics of these two charge-transfer processes for the K51 dye by carrying out transient absorbance measured on the nanosecond time scale. The oxidized Ru(III) complex, with thiocyanate ligands, has a characteristic absorption at $\lambda > 620$ nm. In the absence of a redox mediator, in pure MPN solvent (Figure 3), the decay of the absorption signal, recorded at 680 nm, reflects the dynamics of recombination of injected electrons with the oxidized dye (S^+). The kinetics of S^+ transient absorbance decay for the K51 system show a typical half-reaction time $t_{1/2} = 200$ μs. The half-reaction time being the time lapsed for the absorbance signal to decay to half of its initial value. In the presence of the iodide/triiodide redox electrolyte **A**, the decay of the oxidized dye signal significantly accelerates with $t_{1/2} = 10$ μs. This demonstrates that the back electron transfer is indeed efficiently intercepted in this system. The data for charge recombination kinetics on the mesoscopic TiO_2 film are comparable to what has been reported for the Z907 dye ($t_{1/2} = 180$ μs). [31] However, the decay of the oxidized dye signal due to regeneration of the K51 ($t_{1/2} = 10$ μs) is much faster than that of Z907 ($t_{1/2} = 30$ μs) dye in the same electrolyte. [31] Thus for K51 about 5% of the initial S^+ species recombine with conduction band electrons whereas the loss is 10−15% for Z907.

Table 1. Detailed Device Parameters for K51 Dye with Electrolyte **A** under Various Incident Light Intensities

P_{IN} (mW/cm^2)	J_{SC} (mA/cm^2)	V_{OC} (mV)	P_{MAX} (mW/cm^2)	FF	h (%)
97.7	15.37	738	7.59	0.685	7.8
50.4	8.5	719	4.24	0.728	8.4
29.2	4.99	705	2.53	0.751	8.6

The effect of the potential-determining cation, Li^+, on the decay kinetics of the oxidized dye species was studied in the presence of a fixed concentration of iodide and triiodide. Results of laser kinetic measurements show that, for low concentrations of lithium ions (10^{-2} M) added in the form of $LiClO_4$ in electrolyte **A**, the half-life of the dye regeneration process ($t_{1/2} = 10$ μs) remains constant and is similar to the value obtained with electrolyte **A** with no Li^+ added. Between 10^{-2} and 5×10^{-2} M Li^+, the measured value of $t_{1/2}$ decreases to less than 5 μs and stays approximately constant as the concentration is further increased. A similar behavior was previously observed for N-719 dye-sensitized TiO_2 upon addition of Li^+ and other cations in the electrolytes. [17] It can be rationalized in terms of the global surface charge of the nanocrystalline TiO_2 particles: In the absence of Li^+, or at Li^+ concentrations lower than 10^{-2} M in the electrolyte, the surface of oxide particles is globally negatively charged, due to the adsorption of carboxylated dye molecules. [20] Adsorption of a high concentration of Li^+ to the TiO_2 surface (or the TEOME side chains) confers a globally positive charge to the surface, increasing the local concentration of iodide and hence increasing the dye regeneration rate.

We have measured the current density−voltage (J−V) characteristics of a device based on K51 sensitizer with electrolyte **A**, under air mass (AM) 1.5 simulated sunlight (J−V curves in Supporting Information). Detailed device performances at different light intensities are summarized in Table 1. At 100 mW cm^{-2} the short-circuit current density (J_{sc}), open-circuit voltage (V_{oc}), fill factor (FF), and power conversion efficiency (η) are 15.37 mA cm^{-2}, 738 mV, 0.685, and 7.8%, respectively. Under lower light intensity (30 mW cm^{-2}) AM 1.5 power conversion efficiency is as high as 8.6%. The photovoltaic action spectrum (also shown in Supporting Information) displays a broad spectral response covering almost the entire visible spectrum, with a peak incident photon-to-current quantum efficiency (IPCE) of approximately 80% at a 540 nm incident wavelength.

The photovoltaic performance of K51 is compared with the Z907 dye, which has a similar absorption spectrum and

Table 2. Photovoltaic Parameters of DSCs Based on Z907 and K51 Dyes and Different Electrolytes **A** and **B** (**A** with 0.05 M Li^+), **C** (**A** with 0.125 M Li^+), and **D** (**A** with 0.25 M Li^+) under the AM 1.5 Full Sunlight (100 mW cm^{-2})

sensitizer	electrolyte	V_{oc}/mV	J_{sc}/mA cm^{-2}	FF	η/%
K-51	**A**	738	15.40	0.685	7.80
	B	715	16.60	0.679	8.10
	C	699	16.86	0.675	7.95
	D	681	17.17	0.662	7.75
Z907	**A**	728	12.88	0.704	6.60
	B	678	14.85	0.660	6.65
	C	666	15.2	0.666	6.73
	D	650	14.54	0.65	6.14

molar extinction coefficient. Employing the same electrolyte as above, the efficiency of the Z907 dye is lower (6.6%) due to a decrease in the J_{sc} (12.88 mA cm^{-2}). We attribute the higher photocurrent for devices containing K51 as compared with Z907 to be due to the faster dye regeneration rate observed in the former case.

The influence of various cations (H^+, Li^+, Na^+, K^+, Mg^{2+}, etc.) present in the DSC electrolytes has been thoroughly investigated by others.[17−21] We have obtained interesting results with Z907 and K51 dyes, when various quantities of lithium ions are added to the electrolyte. For cells incorporating Z907 dye in conjunction with electrolyte **B**, the photocurrent increases from 12.88 to 14.85 mA cm^{-2} with increasing lithium ion concentration. However, this is counterbalanced by a decrease in the V_{oc} value from 728 to 678 mV, maintaining the same overall efficiency, Table 2. We attribute the changes in V_{oc} and J_{sc} to the lowering of the TiO_2 conduction band level in the presence of Li^+ ions.[32−34]

Contrary to Z907, cells based on the K51 dye containing TEOME side chains exhibit only small changes in the J_{sc} and V_{oc} upon introducing 50 mM Li^+ in the electrolyte (**B**). The small effect observed suggests that the TEOME side chains of the dye are likely to coordinate to the Li^+ present in the electrolyte, preventing Li^+ from contacting the surface of TiO_2. This explains that the decrease of the V_{oc} is smaller for K51 as compared to Z907. Li^+ scavenging by coordination to the K51 dye is corroborated by the FTIR spectroscopy data shown above.

Higher Li^+ concentrations do significantly affect the J_{sc} and V_{oc} values of devices based on the K51 dye. Results are shown in Figure 4 and Table 2. Increasing the Li^+ concentration from 0.05 to 0.25 M augments the J_{sc} value by 1.8 mA cm^{-2} while the V_{oc} drops by 57 mV. We calculated the amount of Li^+ present in the cell prepared with electrolyte **B** as 5×10^{-8} mol, which is about equal to the amount of dye adsorbed on the surface of the mesoscopic TiO_2 film employed here. It appears that at higher concentrations some lithium ions are not coordinated to the K51 sensitizer and remain free to access the TiO_2 surface lowering the conduction band edge and hence the V_{oc}.

We further extended our studies to solid-state devices that comprise of 2,2′,7,7′-tetrakis(*N*,*N*-di-methoxypheny-amine)-9,9′-spirobifluorene (Spiro-MeOTAD) as a hole transporting material, which replaces the redox liquid electrolyte.[35] Here, we use lithium triflate as an additive to the hole transporter

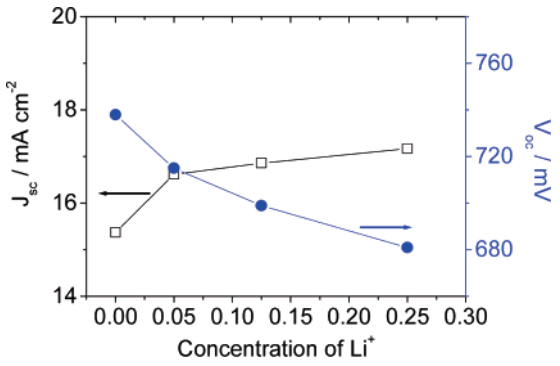

Figure 4. The variations in the J_{sc} and V_{oc} of DSC devices made with K51 dye with electrolytes containing different Li^+ concentrations in M.

as the addition has been shown to dramatically inhibit interfacial charge recombination. Incorporating the "ion coordinating" K51 dye in the solid-state device further slows down the charge recombination rate, resulting in significant improvements to the open-circuit voltage and fill factor, with approximately a 20% increase in device efficiency when comparing K51 to Z907 (3.8% as compared to 3.2%).[4] We previously assigned these improvements to the surface-coordinated ions "screening" the holes in the hole transporter from the electrons in the TiO_2, significantly reducing the charge recombination probability. A further contribution, to the increased open-circuit voltage, is expected to arise from the dipole moment, which may exist at the dye interface due to the permanently adsorbed charged species.[4,36]

Here we consider the effect of lithium adsorption to the TiO_2 surface. Lithium ions are known to be potential determining in TiO_2 due to their ability to adsorb to the surface and intercalate into the TiO_2 anatase crystal structure.[37,38] We have shown evidence above that the K51 dye, when incorporated into a liquid cell, acts to prevent most of the ionic species from adsorbing to the nanoparticle surface. For the solid-state cell we find considerably different behavior for the two dyes when we vary the lithium salt concentration in the hole-transporter solution.

Figure 5 shows the open-circuit voltage plotted against lithium-ion concentration for solid-state devices containing K51 and Z907 dyes. The open-circuit voltage of the K51 device increases constantly with increasing lithium ion concentration, over the range studied. However, for the Z907 device the behavior is much more erratic, with the open-circuit voltage remaining more or less unchanged as the lithium concentration is increased. The charge recombination within devices containing Z907 and other "non ion coordinating" dyes is dramatically reduced with the addition of lithium salts, causing a significant increase in the photocurrent. However, we find that the open-circuit voltage is not greatly improved. This strongly suggests that, although the recombination is reduced, the cationic adsorption to the surface pulls down the potential in the TiO_2, counterbalancing this beneficial effect. For devices containing the ion-coordinating K51 dye, a high concentration of ions is held on the dye molecules and thus causes an increasingly strong "charge screening" effect. This will reduce the charge recombination

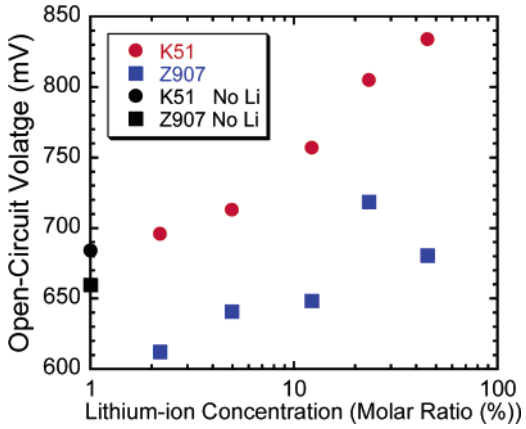

Figure 5. Open-circuit voltage versus concentration of lithium ions for solid-state devices using K51 (red circles) and Z907 (blue squares) as the sensitizing molecules. Lithium triflate is the salt added to the hole-transporter solution, which contains Spiro-MeOTAD and antimony salt as the electronic dopant, in chlorobenzene. The concentration is plotted as molar ratio (%) as compared to Spiro-MeOTAD in the starting solution. Please note that the black markers on the *y*-axis correspond to devices with no lithium (not 1%).

rate and, in this case, increase the open-circuit voltage since the coordinated ions are prevented from adsorbing to the TiO_2 surface and positively shifting the potential.

In conclusion, a novel ion coordinating ruthenium complex NaRu(4-carboxylic acid-4′-carboxylate)(4,4′-bis[(triethylene glycol methyl ether)methyl ether]-2,2′-bipyridine)$(NCS)_2$ has been synthesized and characterized by spectroscopic and electrochemical techniques. We have demonstrated, with FTIR spectroscopy, the ability of this sensitizer to coordinate lithium ions. This "supermolecular complex" performs remarkably well when incorporated in a DSC using a non-volatile electrolyte or hole-transporting material, exhibiting a simulated full-sun power conversion efficiency of 7.8% or 3.8%, respectively. We have demonstrated, for both the liquid and solid-state devices, that K51 dye has an "ion-trapping" functionality, which inhibits the ions from reaching the TiO_2 surface. Hence, in a liquid electrolyte device there is little reduction in open-circuit voltage, and for the solid-state device there is a significant increase in the open-circuit voltage, when Li^+ is added. Future work is under way to extend this concept of incorporating ion coordinating side chains or crown ethers on molecules with larger π-conjugated systems. This should result in enhanced light-harvesting efficiency and thus higher photon-to-electron conversion efficiencies.

Acknowledgment. We are grateful to Dr. P. Wang for helpful discussions and R. T. Koyanagi (CCIC, Japan) for providing the 400 nm sized TiO_2 particles. The Swiss Science Foundation and Swiss Federal Office for Energy (OFEN) and the European MOLYCELL project (OFES 03.0681-1) have supported this work.

Supporting Information Available: The synthesis, cyclic voltammogram curve, electronic absorption and emission spectra of the K51 sensitizer, and $J-V$ IPCE curves of the device. This material is available free of charge via the Internet at http://pubs.acs.org.

References

(1) Grätzel, M. *Chem. Lett.* **2005**, *34*, 8.
(2) O'Regan, B.; Grätzel, M. *Nature* **1991**, *353*, 737.
(3) Grätzel, M. *Nature* **2001**, *414*, 338.
(4) Snaith, H. J.; Zakeeruddin, S. M.; Schmidt-Mende, L.; Klein, K.; Grätzel, M. *Angew. Chem., Int. Ed.* **200**5, *44*, 6413.
(5) Ito, S.; Liska, P.; Comte, P.; Charvet, R.; Pechy, P.; Bach, U.; Schmidt-Mende, L.; Zakeeruddin, S. M.; Kay, A.; Nazeeruddin, M. K.; Graetzel, M. *Chem. Commun.* **2005**, *34*, 4351.
(6) Grätzel, M. *Inorg. Chem.*, **2005**, *44* (20), 6841
(7) Nazeeruddin, M. K.; Pechy, P.; Renouard, T.; Zakeeruddin, S. M.; Humphry-Baker, R.; Liska, P.; Cevey, L.; Costa, E.; Shklover, V.; Spiccia, L.; Deacon, G. B.; Bignozzi C. A.; Grätzel, M. *J. Am. Chem. Soc.* **2001**, *123*, 1613.
(8) Wang, P.; Klein, C.; Humphry-Baker, R.; Zakeeruddin, S. M.; Grätzel, M. *J. Am. Chem. Soc.* **2005**, *127*, 808.
(9) Wang, P.; Klein, C.; Humphry-Baker, R.; Zakeeruddin, S. M.; Grätzel, M. *Appl. Phys. Lett.* **2005**, *86*, 123508.
(10) Wang, P.; Zakeeruddin, S. M.; Moser, J.-E; Humphry-Baker, R.; Compte. P; Nazeeruddin, M. K; Grätzel, M. *Adv. Mater.* **2004**, *16* (20), 1806.
(11) Wang, P.; Humphry-Baker, R.; Zakeeruddin, S. M.; Moser, J.-E.; Grätzel, M. *Chem. Mater.* **2004**, *16*, 3246.
(12) Hara, K.; Kurashige, M.; Kan-oh, Y.; Kasada, C.; Shinpo, A.; Suga, S.; Sayama, K.; Arakawa, H. *New J. Chem.* **2003**, *27*, 783.
(13) Horiuchi, T.; Miura, H.; Sumioka, K.; Uchida, S. *J. Am. Chem. Soc.* **2004**, *126*, 12218.
(14) Wang, Z. S.; Hara, K.; Sato, T.; Dan-oh, Y.; Kasada, C.; Shinpo, A.; Suga, S.; Arakawa, H.; Sugihara, H. *J. Phys. Chem. B* **2005**, *109*, 3907.
(15) Islam, A.; Chowdhury, F. A.; Chiba, Y.; Komiya, R.; Fuke N,; Ikeda, N.; Han, L, *Chem. Lett.* **2005**, *34*(3), 344.
(16) Sauve, G.; Cass, M. E.; Doig, S. J.; Lauemann, I.; Pomykal, K.; Lewis, N. S. *J. Phys. Chem. B* **2000**, *104*, 3488.
(17) Pelet, S.; Moser, J.-E; Grätzel, M. *J. Phys. Chem. B* **2000**, *104*, 1791.
(18) Nakade, S.; Kambe, S.; Kitamura, T.; Wada, Y.; Yanagida, S. *J. Phys. Chem. B* **2001**, *105*, 9150.
(19) Nakade, S.; Kanzaki, T.; Kubo, W.; Kitamura, T.; Wada, Y.; Yanagida, S. *J. Phys. Chem. B* **2005**, *109*, 3480.
(20) Kambe, S.; Nakade, S.; Kitamura, T.; Wada, Y.; Yanagida, S. *J. Phys. Chem. B* **2002**, *106*, 2967.
(21) Frank, A. J.; Kopidakis, N.; van de Lagemaat, J. *Coord. Chem. Rev.* **2004**, *248*, 1165.
(22) Kim, J. H.; Kang, M. S.; Kim, Y. J.; Won, J. Park, N. G.; Kang, Y. S. *Chem. Commun.* **2004**, 1662.
(23) Kang, M. S.; Kim, J. H.; Kim, Y. J.; Won, J. Park, N. G.; Kang, Y. S. *Chem. Commun.* **2005**, 889.
(24) Barbé, C. J.; Arendse, F.; Comte, P.; Jirousek, M.; Lenzmann, F.; Shklover, V.; Grätzel, M. *J. Am. Ceram. Soc.* **1997**, *80*, 3157.
(25) Wang, P.; Zakeeruddin, S. M.; Comte, P.; Charvet, R.; Humphry-Baker, R.; Grätzel, M. *J. Phys. Chem. B* **2003**, *107*, 14336.
(26) Wang, P.; Bernard, W.; Humphry-Baker, R.; Moser, J.-E; Teucher, J.; Kantlehner, W.; Mezger, J.; Stoyanov, E. V.; Zakeeruddin, S. M.; Comte, P.; Charvet, R.; Grätzel, M. *J. Am. Chem. Soc.* **2005**, *127*, 6850.
(27) Schmidt-Mende, L.; Zakeeruddin, S. M.; Graetzel, M. *Appl. Phys. Lett.* **2005**, *86*, 013504.
(28) Allen, G. H.; White, R. P.; Rillema, D. P.; Meyer, T. J. *J. Am. Chem. Soc.* **1984**, *106*, 2613.
(29) Duffy, N. W.; Dobson, K. D.; Gordon, K. C.; Robinson, B. H.; MeQuillan, A. *J. Chem. Phys. Lett.* **1977**, *266*, 451.
(30) Wieczorek, W.; Lipka, P.; Zukowska, G.; Wycislik, H. *J. Phys. Chem. B* **1998**, *102*, 6968.
(31) Wang, P.; Zakeeruddin, S. M.; Moser, J.-E; Nazeeruddin, M. K.; Sekiguchi, T.; Grätzel, M. *Nat. Mater.* **2003**, *2*, 402.
(32) Redmond, G.; Fitzmaurice, D. *J. Phys. Chem.* **1993**, *97*, 1426.
(33) Enright, B.; Redmond, G.; Fitzmaurice, D. *J. Phys. Chem.* **1994**, *98*, 6195.
(34) Lindstrom, H.; Sodergren, S.; Solbrand, A.; Rensmo, H.; Hjelm, J.; Hagfeldt, A.; Lindquist, S.-E. *J. Phys. Chem. B* **1997**, *101*, 7717.
(35) Bach, U.; Lupo, D.; Comte, P.; Moser, J.-E; Weissörtel, F.; Salbeck, J.; Spreitzer, H.; Grätzel, M. *Nature* **1998**, *395*, 583.
(36) Kruger, J.; Bach, U.; Grätzel, M. *Adv. Mater.* **2000**, *12*, 447.
(37) Huang, S. Y.; Kavan, L.; Exnar, I.; Grätzel, M. *J. Electrochem. Soc* **1995**, *142*, L142.
(38) Lunell, S.; Stashans, A.; Ojamae, L.; Lindstrom, H.; Hagfeldt, A. *J. Am. Chem. Soc.* **1997**, *119*, 7374.

NL060075M